AD-A152 374 PROTONATION AND LEWIS ACID-BASE EQUILIBRIA IN (BIPYRAZINE)MOLYBDENUM AND (..(U) YORK UNIV DOWNSVIEW (ONTARIO) DEPT OF CHEMISTRY E S DODWORTH ET AL. MAR 85 1/1

UNCLASSIFIED TR-35 N00014-78-C-0592 F/G 7/4 NL

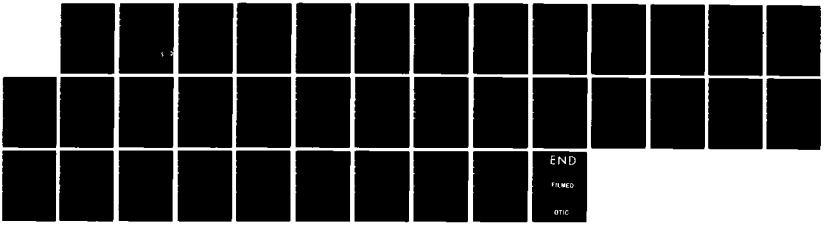

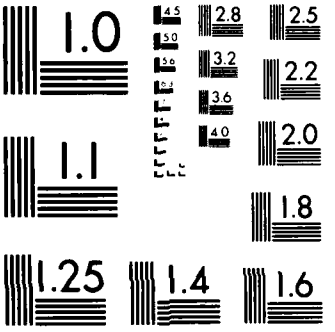

(2)

OFFICE OF NAVAL RESEARCH

Contract N00014-78-C-0592

Task No. NR 051-693

TECHNICAL REPORT NO. 35

Protonation and Lewis Acid-Base Equilibria in (Bipyrazine)Molybdenum and (Bipyrazine)Tungsten Tetracarbonyls

BY

Elaine S. Dodsworth, A.B.P. Lever, Goran Eryavec and Robert J. Crutchley

Prepared for Publication

in

Inorganic Chemistry

York University

Department of Chemistry

Downsview (Toronto)

Ontario M3J-1P3

SECURITY CLASSIFICATION OF THIS PAGE (When Data Entered)

REPORT DOCUMENTATION PAGE

READ INSTRUCTIONS BEFORE COMPLETING FORM

1. REPORT NUMBER: Technical Report No. 35
2. GOVT ACCESSION NO.: A152 374
3. RECIPIENT'S CATALOG NUMBER:

4. TITLE (and Subtitle): Protonation and Lewis Acid-Base Equilibria in (Bipyrazine)Molybdenum and (Bipyrazine)Tungsten Tetracarbonyls

5. TYPE OF REPORT & PERIOD COVERED:

6. PERFORMING ORG. REPORT NUMBER:

7. AUTHOR(s): Elaine S. Dodsworth, A.B.P. Lever, Goran Eryavec and Robert J. Crutchley

8. CONTRACT OR GRANT NUMBER(s): N00014-78-C-0592

9. PERFORMING ORGANIZATION NAME AND ADDRESS: York University, Chemistry Department, 4700 Keele St., Downsview, Ontario M3J 1P3 Canada

10. PROGRAM ELEMENT, PROJECT, TASK AREA & WORK UNIT NUMBERS:

11. CONTROLLING OFFICE NAME AND ADDRESS:

12. REPORT DATE: March, 1985

13. NUMBER OF PAGES: 28

14. MONITORING AGENCY NAME & ADDRESS (if different from Controlling Office):

15. SECURITY CLASS. (of this report): Unclassified

15a. DECLASSIFICATION/DOWNGRADING SCHEDULE:

16. DISTRIBUTION STATEMENT (of this Report)

THIS DOCUMENT HAS BEEN APPROVED FOR PUBLIC RELEASE AND SALE;

ITS DISTRIBUTION IS UNLIMITED

Accession For
NTIS GRA&I [X]
DTIC TAB [ ]
Unannounced [ ]
Justification
By
Distribution/
Availability Codes
Dist | Avail and/or Special
A-1

17. DISTRIBUTION STATEMENT (of the abstract entered in Block 20, if different from Report)

18. SUPPLEMENTARY NOTES

Prepared for publication in the Journal of Inorganic Chemistry

19. KEY WORDS (Continue on reverse side if necessary and identify by block number)

Bipyrazine, Molybdenum, Tungsten, Carbonyl, Acid-base, Electronic spectra

20. ABSTRACT (Continue on reverse side if necessary and identify by block number)

The title complexes react with boron trifluoride etherate to generate mono- and di-BF_3 adducts. In H_2SO_4/ethanol solution one proton is coordinated. In each case reaction is assumed to occur at the peripheral uncoordinated nitrogen atoms of the bipyrazine unit. New metal to ligand charge transfer bands are observed for these various species. Analysis of the spectra shows that $pK_a(1)$ for the first uncoordinated nitrogen atom is about -0.3(Mo complex), and that extensive mixing of ground and excited states must be occurring to account for the oscillator strengths and bandwidths observed.

DD FORM 1 JAN 73 1473 EDITION OF 1 NOV 65 IS OBSOLETE
S/N 0102-014-6601

Contribution from the Dept. of Chemistry, York University, Downsview (Toronto), Ontario, Canada M3J 1P3

Protonation and Lewis Acid-Base Equilibria in (Bipyrazine)Molybdenum and (Bipyrazine)Tungsten Tetracarbonyls

By Elaine S. Dodsworth, A.B.P. Lever*, Goran Eryavec and Robert J. Crutchley

Abstract

The title complexes react with boron trifluoride etherate to generate mono- and di-BF_3 adducts. In H_2SO_4/ethanol solution one proton is coordinated. In each case reaction is assumed to occur at the peripheral uncoordinated nitrogen atoms of the bipyrazine unit. New metal to ligand charge transfer bands are observed for these various species. Analysis of the spectra shows that $pK_a(1)$ for the first uncoordinated nitrogen atom is about -0.3(Mo complex), and that extensive mixing of ground and excited states must be occurring to account for the oscillator strengths and bandwidths observed.

Introduction

Ground and excited state protonation equilibria involving the $Ru(bpz)_3^{2+}$ ion (bpz = bipyrazine) have recently been reported.[1] This species binds up to six protons in a step-wise fashion providing an interesting series of electronic absorption and emission data. Of especial interest was the variation in metal to ligand charge transfer (MLCT) energy as a function of the degree and site of protonation. Step-wise protonation provides a useful

mechanism for 'tuning' excited state redox potentials[2] and is of obvious interest in the design of photocatalytic redox reagents. Previous studies of protonation equilibria involving inorganic complexes have discussed protonation at the nitrogen atom of coordinated cyanide ion in species such as $M(CN)_4L$ and $M(CN)_2L_2$ (M = Fe, Ru; L = di-imine)[3,4], considered the enhanced acidity of ruthenium(II) complexes of 4,7-dihydroxy-1,10-phenanthroline[5], and analysed the pH dependence of ruthenium bipyridine[6] and bipyrimidine[7] species. As is evident, much of the work has been associated with ruthenium or its congeners. The binding of Lewis acids to cyanide complexes and its effect on their charge transfer spectra has also been studied.[8] For these reasons we considered it useful to probe the protonation equilibria in a complex other than ruthenium and having only one bipyrazine unit to provide a data set which might be capable of more detailed analysis and additional insights.

The species $M(CO)_4(bpz)$ (M = Mo, W)[9] are soluble in organic solvents and give rise to intense absorption in the visible region, attributed to metal to ligand charge transfer (MLCT) M→bpz(π^*). Addition of mineral acid, or the Lewis acid BF_3 (etherate) causes changes in the visible absorption spectra which can be interpreted in terms of mono- and di-acid equilibria. FTIR and NMR data are reported in support of the equilibria proposed.

Experimental

The complexes $Mo(CO)_4(bpz)$ and $W(CO)_4(bpz)$ were prepared according to literature methods.[9] Acetone and 96% H_2SO_4 were BDH Analar grade. The acid was diluted using absolute ethanol. Boron trifluoride etherate was purified

according to a literature method[10] and stored under nitrogen or dry air. Electronic spectra were recorded on a Perkin-Elmer Hitachi Model 340 microprocessor spectrophotometer. The cell holder was cooled to ca. 10°C to minimise decomposition of the complexes. ^{1}H NMR spectra were recorded on a Varian EM360 60 MHz spectrometer at ambient temperature. Tetramethylsilane at 0.00 ppm or the residual protons of d_6-acetone at 2.05 ppm were used as internal references. FTIR spectra were recorded on a Nicolet SX20 instrument, (courtesy of the Nicolet Co. of Canada) as acetone solutions in a sodium chloride cell. Computer simulations were obtained with a Commodore model 8032 microcomputer and an Epson MX80 matrix printer utilised in a plotting mode.

Results and Discussion

The visible absorption spectra of the title species show two bands in the visible region, bands I and II (Tables I and II). These transitions have been studied previously[9,11-16] and are clearly associated with $M(t_{2g}^6) \rightarrow bpz(b_2\pi^*)$ (MLCT I) and $M(t_{2g}^6) \rightarrow bpz(a_2\pi^*)$ (MLCT II), being transitions from the metal d shell to the two lowest lying π^* orbitals of bpz. These are separated by some 7000-8000 cm^{-1}.

The species show marked solvatochromic behaviour with the two MLCT transitions shifting to the blue by up to 3000 cm^{-1} as the dielectric constant of the solvent is increased[16], behaviour similar to the corresponding bipyridine (bipy) complexes.[11,12] There is indeed a simple linear correlation between the shifts of the MLCT transitions in $M(CO)_4$(bipy) with solvent, and those of the complexes under study here.[16] The presence of the two peripheral nitrogen atoms, absent in the bipyridine

species, was expected to cause deviations in the linear relationship between the two series, when acidic solvents were considered.

As far as glacial acetic acid and trichloroacetic acid (in ethanol) are concerned, no marked differences were noted and presumably protonation does not occur in these media. However, while the addition of mineral acids, HCl, $HClO_4$ and H_2SO_4, to an ethanolic solution of $M(CO)_4(bipy)$ causes only small solvatochromic shifts (to the blue) in the MLCT band energies, addition to $M(CO)_4(bpz)$ causes new bands to be observed.

Solutions of HCl, $HClO_4$, and H_2SO_4 in either water or ethanol cause gradual decomposition of the complexes, as indicated by a decrease in the intensity of the MLCT bands with time. The rate of decomposition increases with increasing acid concentration, being significant within minutes in 4M acid. We were not able to identify an acid system which was free of decomposition effects. Such decomposition also continues under an inert atmosphere (CO, N_2). Solutions of H_2SO_4 in ethanol were finally chosen for further study of the protonation since the complexes are readily soluble in this solvent, and decomposition is very slow at low acidities (<3M). Although some esterification must take place in the mixed $EtOH/H_2SO_4$ medium, it does not seem to be a problem for our study, except that the proton concentration will be uncertain.

Addition of the Lewis acid, BF_3 (as boron trifluoride etherate), to solutions of the bpz complexes causes spectroscopic effects apparently similar to those of protonation. In both experiments the results for Mo and W complexes are qualitatively the same.

When boron trifluoride etherate is added dropwise to the, initially,

pink solution of $M(CO)_4(bpz)$ (M = Mo,W) in acetone, bands I (MLCT I) and II (MLCT II) diminish in intensity, and a new band (band Ia) appears at about 618 nm, shifting to lower energy with continued addition of the BF_3. Subsequently, at higher concentrations of the etherate, bands I and II essentially disappear and there remain band Ia and a new band at about 490 nm (band Ib). In pure boron trifluoride etherate as solvent, only bands Ia and Ib are seen, the latter being the more intense. These data are summarised in Table I and Fig. 1. When the solution is diluted, band Ib diminishes in intensity and bands I and II of the parent species reappear. Thus the reaction seems quite reversible with little or no decomposition.

Band Ia is associated with MLCT I of the mono-BF_3 adduct and band Ib with MLCT I of the di-BF_3 adduct. There is no evidence in the data obtained here for bands corresponding to MLCT II appearing in either adduct (at least to the red of the parent transition). The red shifting of band Ia, upon further addition of BF_3 etherate, probably reflects a solvatochromic effect, expected to shift this transition to lower energies as the polar acetone is diluted with the less polar diethyl-ether.[14]

Attempts to isolate a solid adduct from reaction of $Et_2O.BF_3$ with $Mo(CO)_4bpz$ or $W(CO)_4bpz$ were unsuccessful; reactions of the solids with liquid $Et_2O.BF_3$ (at room temperature, in vacuo) produced black oils.

Data for protonation of $Mo(CO)_4bpz$ and $W(CO)_4bpz$ are presented in Table II and typical spectra are shown in Fig. 2. As the acidity of the solution is increased a new peak (band Ia) appears in the spectrum, red shifted with respect to MLCT I. Isosbestic points are observed at 586 and 584 nm for Mo

and W species respectively. Band Ia continues to increase in intensity (and also red shifts slightly), while MLCT I decreases. Above about 1.5M acid, the isosbestic point is lost, probably because decomposition is beginning to occur. Band I decreases to a shoulder in 2.5M H_2SO_4. Above this concentration a second new band (Ib) appears close to the position of MLCT I but significantly blue shifted. This band then increases in intensity relative to band Ia. At acid concentrations greater than 4M the rate of decomposition of the complex becomes significant relative to the time taken to record the spectrum; thus the investigation could not be continued.

The effect of acid on MLCT II, the $d \rightarrow a_2\pi^*$ transition, is less easily observed due to its proximity to stronger bands in the UV region (bpz $\pi \rightarrow \pi^*$ and M→CO MLCT) though it does show a decrease in intensity roughly parallel with MLCT I. No new bands are observed close to MLCT II. This absorption feature disappears altogether from the spectrum in >4M (Mo) and >3.25M (W) H_2SO_4.

When acid solutions ($[H^+]<1M$) are diluted or neutralised, bands I and II reappear and band Ia diminishes. However, if stronger acid solutions, in which band Ib is present, are diluted or neutralised, the reversal is incomplete and the spectra are broad in the region of band I. Furthermore if a solution in fairly strong acid is monitored with time, band Ib <u>increases</u> slightly over short time intervals (minutes) as band Ia decreases. This increase is not associated with growth in band II and cannot therefore reflect an increase in the concentration of the parent complex. Over longer time periods both bands Ia and Ib diminish. We return to this problem below.

Tetracarbonyldi-imine complexes of C_{2v} symmetry have four allowed CO

stretching modes in their IR spectra: A_1, B_1, A_1 and B_2. In $Mo(CO)_4bpz$ the two higher frequency bands correspond primarily to the trans carbonyls and the two lower bands primarily to the cis carbonyls.[9,17,18] FTIR spectra of the CO stretching region and corresponding electronic spectra were recorded for solutions of $Mo(CO)_4bpz$ in acetone and in the presence of varying amounts of $Et_2O.BF_3$. Apart from some broadening of the CO bands as BF_3 was added, there was no significant change in the spectrum during the growth of band Ia. When there was added a sufficient excess of $Et_2O.BF_3$ corresponding to the appearance of band Ib in the electronic spectrum, the energies of all four ν(CO) increased (Table III).

Assignments of the parent carbonyl spectrum (Table III) have already been discussed.[9]. As expected for the CO band force constants, k_1 (CO groups trans to di-imine) < k_2 (CO groups perpendicular to di-imine plane). We anticipate that boron trifluoridation will increase the acceptor power of the di-imine and lead to an increase in both k_1 and k_2. The assignment shown in Table III for the BF_3 adduct fulfills this expectation though the fit to the Kraihanzel-Cotton matrices[18] is not quite as good as for the parent species. This poorer fit probably reflects the fact that the dominant species in solution is the mono-adduct which possesses at best C_s symmetry, rather than the C_{2v} symmetry assumed by the theoretical analysis. Other assignments provide even poorer fits to the matrices or result in $k_1 > k_2$. This would imply that $bpzBF_3$ is a better acceptor than CO which is an improbable result.

Note that these data permit one to derive the ligand effect constants defined by Timney for deducing carbon monoxide stretching force constants.[19]

The bpz and BF_3 adduct may be compared with bipyridine and CO, as follows:-

	Cis constant	Trans constant
bipy	$-24\ N\ m^{-1}$	$-62\ N\ m^{-1}$
bpz	-13.5	-59
$bpzBF_3$	-5	-52.5
CO	33.5	126.1

The variation is consistent with the ligands becoming better π-acceptors in the sequence bipy < bpz <$bpzBF_3$<<CO.

^1H NMR spectra were recorded in acetone (d_6) solution and in the presence of an excess of $Et_2O.BF_3$ (Table IV). The complex itself shows three resonances in the aromatic region.[9] On addition of $Et_2O.BF_3$ the same three resonances are observed, recognisable by their splitting patterns, but H3 and H6 are shifted downfield (H6 shows around twice the shift of H3) while H5 remains at almost the same position. These shifts can be interpreted in terms of a combination of several effects, as discussed by Martin et al.[20] who have recently reported the ^1H NMR spectra of a series of substituted pyridines and their BF_3 and BBr_3 adducts.

The CO stretching frequency data for $Mo(CO)_4$bpz (see above) indicate that the electron density on the metal decreases when the BF_3 adduct is formed. This may be due to either weaker σ donation from the bpz or to increased π back-donation to the bpz, either one of which will add to the net deshielding of proton H6. Increased back-donation (and thus a net increase in ring current) seems more probable since this may explain why H3 shifts downfield when H5 does not, H3 being in a stronger field due to the π electrons of both rings.

The NMR data for BF_3 addition appear to indicate that only one

(symmetric) species is present in solutions containing an excess of $Et_2O.BF_3$. Since the reaction is reversible, it is possible that the rate of exchange of BF_3 is fast on the NMR time scale so that an average signal is seen, due to the equilibrium between the mono- and di-BF_3 species.

The above results are interpreted in terms of a series of equilibria between the complex and the mono and di-adduct species. For example, in the case of protonation:

$$M(CO)_4bpz \overset{H^+}{\rightleftharpoons} [M(CO)_4bpzH]^+ \overset{H^+}{\rightleftharpoons} [M(CO)_4bpzH_2]^{2+}$$

Band Ia is attributed to the MLCT transition in the monoprotonated complex. It increases in intensity as the acid concentration is increased and the equilibrium moves to the right, while bands I and II, due to the neutral species, decrease.

Approximate pK_a values may be calculated for the first protonation step where isosbestic points are present in the spectra. Values obtained at 283K (assuming $[H^+] = [H_2SO_4]$) are around -0.3 for Mo and +0.1 for W complexes, though there is some variation in the apparent pK_a with acid concentration (due to experimental error and to other equilibria between the acid and solvent). These values are reasonable, lying between those of free bpz (pK_a = 0.45) and $[Ru(bpz)_3]^{2+}$ (pK_a = -2.2)[1]. Although bonding to metal(0) might be expected to increase the pK_a of bpz, evidently back-bonding to the CO groups takes most of the M(0) π electron density.

The molecular orbitals of bipyrazine may be constructed by combining the orbitals of two pyrazine units in and out-of-phase, resulting in a low lying π^* orbital of b_2 symmetry and a higher lying π^* orbital of a_2 symmetry. This latter orbital is constructed of the a_u π^* orbital of pyrazine (in

D_{2h} symmetry), which possesses a nodal plane through the two nitrogen atoms.[21] It is likely that the dominant contribution to the bipyrazine a_2 π^* state also possesses nodal planes through the nitrogen atoms, providing a partial explanation of the differing effects of the initial protonation (or boron trifluoridation) upon the two MLCT transitions.

In the neutral species, the b_2 π^* orbital is symmetrically delocalised over the whole bipyrazine unit. In the monoprotonated species, this orbital will be stabilised by addition of a proton. A protonated bipyrazine unit may be created by combining pyz with $pyzH^+$. Although the symmetry is now lowered to C_s, two molecular orbitals corresponding to the original b_2 π^* and a_2 π^* of the neutral ligand are still obtained and we continue to use the same labels. The atomic orbital contributions to the molecular orbitals will be such that the $pyzH^+$ moiety will contribute primarily to the lower energy b_2 π^*, while the a_2^* state is probably less perturbed and will still be roughly equally delocalised. The state corresponding to band Ia will therefore involve an electron localised mainly in the protonated pyrazine ring. Compare, for example, the red shift observed on protonation of pyrazine in $[Ru(NH_3)_5(pyz)]^{2+}$.[22] The metal d orbitals are also expected to be stabilised somewhat as the protonated bpz becomes a stronger π acceptor (see below). The net red shift then corresponds to the difference in stabilisation of the metal and ligand (b_2 π^*) orbitals.

The first nitrogen atom to be protonated in an excited bipyrazine unit is more basic in the excited state than in the ground state, due to the presence of the excited electron, resulting in a red shift of the MLCT transition (Forster).[23] The second excited state (MLCT II) is not a stronger

Fig 1

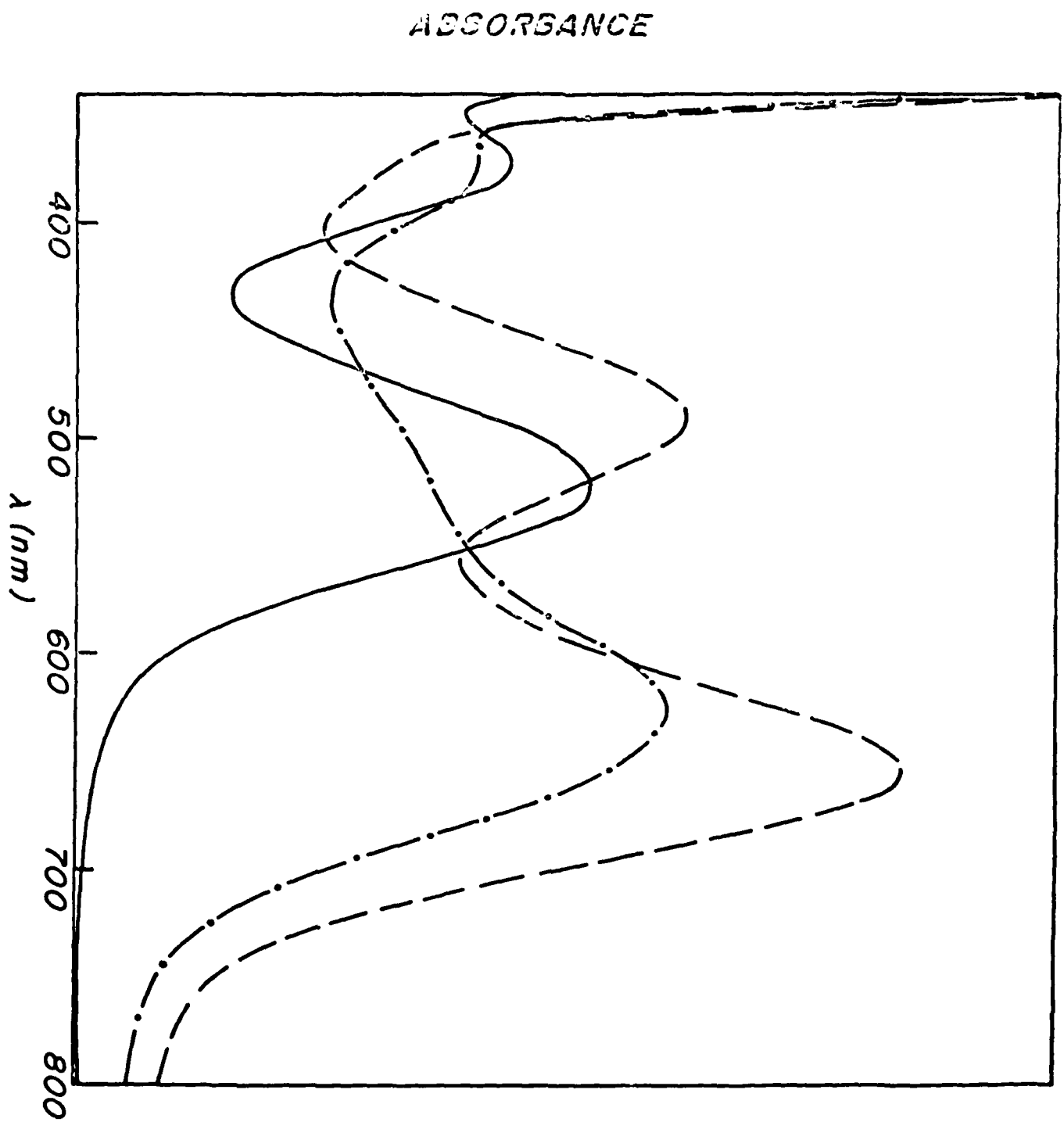

FIGURE LEGENDS

Figure 1

Visible absorption spectra of $Mo(CO)_4bpz$ showing the effect of $Et_2O.BF_3$ addition. _____ Initial spectrum in acetone. -·-·- Predominant species = $Mo(CO)_4bpz.BF_3$. --- Limiting spectrum corresponding (mainly) to

$$Mo(CO)_4bpz.BF_3 \quad \overset{Et_2O.BF_3}{} \quad Mo(CO)_4bpz.2BF_3$$

Figure 2

(a) Visible absorption spectra of $1x10^{-4}$M $Mo(CO)_4bpz$ in H_2SO_4/ethanol as a function of $[H_2SO_4]$. Curves 1-5 correspond to $[H_2SO_4]$ of 0, 0.5, 0.75, 1.0 and 1.25 mol l^{-1} respectively.
(b) As (a) with $[H_2SO_4]$ = 1.5M _____, 2.0M -.-.-.-, 2.5M -----.

Figure 3

The simulated electronic spectra of $Mo(CO)_4bpz$ and its monoprotonated derivative. The spectra correspond with Fig. 2 (a) with the following percentage composition reading from the top spectrum at 377nm down. (i) 100% parent unprotonated; (ii) 92% parent, 8% monoprotonated; (iii) 86% parent, 14% monoprotonated; (iv) 81.55% parent, 17.95% monoprotonated, 0.5% 'diprotonated'; (v) (and lowest at 377 nm) 75% parent, 24% monoprotonated, 1% 'diprotonated'. The molar absorbances and bandwidths are as indicated in Table V; gaussian band shape was simulated.

Figure 4

The gaussian construction of the spectrum labelled (v) in Fig. 3. The dotted lines correspond with the parent species, the circles to the monoprotonated species, and the crosses to the 'diprotonated' species.

Table V Spectroscopic Parameters

	Solvent		Transition	Energy (ε)	Half Bandwidth	Oscillator Strength
$Mo(CO)_4bpz$	A		MLCT I	18,300(7400)	2880	0.10
			MLCT Ix	20,700(<2000)[a]	2880[a]	<0.03
			MLCT II	26,530(6160)	4550	0.13[b]
$Mo(CO)_4bpz$	B		MLCT I	19,230	3260	
			MLCT II	27,130	6200	
$Mo(CO)_4(bpzH)^+$	A	(Ia)	MLCT I	15,650(12,580)	2340	0.13
$Mo(CO)_4(bpzBF_3)$	C	(Ia)	MLCT I	15,400	2300	
$Mo(CO)_4(bpz(BF_3)_2)$	C	(Ib)	MLCT I	20,400	6000	
$W(CO)_4bpz$	A		MLCT I	17,920(9280)	2400	0.10
			MLCT II	26,200(6670)	3800	0.12[b]
$W(CO)_4bpz$	B		MLCT I	18,800	2800	
			MLCT II	27,000		
$W(CO)_4(bpzH)^+$	A	(Ia)	MLCT I	15,750	1900	
$W(CO)_4(bpzBF_3)$	C	(Ia)	MLCT I	15,630	1850	
$W(CO)_4(bpz(BF_3)_2)$	C	(Ib)	MLCT I	20,400	4060	

A = EtOH, B = Acetone, C = Acetone/Ether/BF_3 Data in cm^{-1}.

a) Estimated from deconvoluting MLCT I and MLCT Ix and fitting spectra.

b) Approximate; includes some contribution from uv region.

Table IV. ^1H NMR Spectra of $Mo(CO)_4bpz$ and $W(CO)_4bpz$[a]

	H3	H5	H6
$Mo(CO)_4bpz$	10.05	8.90	9.27
+ $Et_2O.BF_3$ (excess)	10.42	8.97	10.14
$W(CO)_4bpz$	10.08	8.85	9.35
+ $Et_2O.BF_3$ (excess)	10.41	8.80	10.19

(a) Data in ppm from Me_4Si. Recorded in d_6 acetone.

Table III Carbonyl Stretching Frequencies and Force Constants[a]

	A_1	B_1	A_1	B_2	k_1	k_2	k_i	A_1 (calc).
$Mo(CO)_4bpz$	2020	1919	1896	1851	14.17	15.55	0.34	1890
+ $Et_2O.BF_3$[b]	2024	1934[c]	1921[c]	1863	14.32	15.72	0.31	1890

a) Vibrational frequencies cited in cm^{-1}, force constants in millidynes/Å. Solvent acetone. b) Note that the dominant species in the presence of excess $Et_2O.BF_3$ is the mono-BF_3 adduct; however, some di-adduct will be present. c) The assignments of the 1934 and 1921 vibrations may be reversed. The reverse assignment leads to k_1 = 14.36, k_2 = 15.60, k_i = 0.35 md/A., A_1(calc.) = 1891 cm^{-1}.

Table II. (a) Spectroscopic Data for $Mo(CO)_4bpz$ in Ethanol/H_2SO_4

Concn. of H_2SO_4 (mol l^{-1})	Band II		Band I/Ib		Band Ia	
	λ_{max}(nm)	ε	λ_{max}(nm)	ε	λ_{max}(nm)	ε
0	377	6180	547	7430		
0.5	377	5880	542	6870	(sh)	
1.0	377	5350	542	6080	630	3340
1.5	377	5270	542	5610	634	4950
2.0	377	4800	546	5080	637	6560
2.5	377	4520	548(sh)	4850	640	7680
3.0	377	3800	540(sh)	4800	642	8860
3.5	376(sh)	3420	522	5980	647	9700
4.0	376(sh)	2660	522	7410	658	9630

(b) Spectroscopic Data for $W(CO)_4bpz$ in Ethanol/H_2SO_4

Concn. of H_2SO_4 (mol l^{-1})	Band II		Band I/Ib		Band Ia	
	λ_{max}(nm)	ε	λ_{max}(nm)	ε	λ_{max}(nm)	ε
0	380	6670	558	9280		
0.5	379	6470	554	8520	(sh)	
1.0	379	5980	556	7650	628	6600
1.5	379	4870	557	6700	631	8590
2.0	379	4690	560(sh)	6230	633	10280
2.5	380	4320	520,540(sh)	5720,6180	634	12320
3.0	380(sh)	3510	502,520(sh)	6960,6910	636	12620
3.5			506	9370	640	12910
4.0			503	10510	644	11680

ε = molar absorbance (1 mol^{-1} cm^{-1}). (sh) = shoulder

Molar absorbances are not corrected for decomposition. Spectra were recorded immediately after mixing and errors are <2% for 2M H_2SO_4 and <5% for 4M H_2SO_4.

Table I. Electronic Spectra of $M(CO)_4bpz$ in the Presence of $Et_2O.BF_3$

Approx. Concn. of $Et_2O.BF_3$ (mol l^{-1})	Colour	$Mo(CO)_4bpz$ λ_{max}(nm) II	I/Ib	Ia	$W(CO)_4bpz$ λ_{max}(nm) II	I/Ib	Ia
0	pink	368.5	520		371	533	
0.07	pink	369	523	(sh)	371	534	(sh)
0.13	mauve	370	527	618	371	539	616
0.17	blue	371	(sh)	625	371	(sh)	620
0.20	blue	371	494	640	(sh)	482	630
0.33	grey-blue	(sh)	490	653	-	480	640
7.9[a]	grey-blue				322	490	654

Spectra recorded using approx. 10^{-4}M $M(CO)_4bpz$ in acetone. Solutions were deoxygenated with dry N_2 before addition of $Et_2O.BF_3$. (a) Complex dissolved in pure $Et_2O.BF_3$.

(17) Adams, D.M., "Metal-Ligand and Related Vibrations", Arnold, E., London, **1967**, p.101.

(18) Kraihanzel, C.S., Cotton, F.A., Inorg. Chem., **1963**, 2, 533. Cotton, F.A., Kraihanzel, C.S., J. Am. Chem. Soc., **1962**, 84, 4432.

(19) Timney, J.A., Inorg. Chem., **1979**, 18, 2502.

(20) Martin, D.R., Mondal, J.U., Williams, R.D., Iwamoto, J.B., Massey, N.C., Nuss, D.M., Scott, P.L., Inorg. Chim. Acta., **1983**, 70, 47.

(21) Jorgenson, W.L., Salem, L., "The Organic Chemists Book of Orbitals", Academic Press, **1973**.

(22) Ford, P., Rudd, De F.P., Gaunder, R., Taube, H., J. Am. Chem. Soc., **1968**; 90, 1187.

(23) Ireland, J.F., Wyatt, P.A.H., Adv. Phys. Org. Chem., **1976**, 12, 131.

(24) Staal, L.H., Stufkens, D.J., Oskam, A., Inorg. Chim. Acta., **1978**, 26, 255.

(25) Lever, A.B.P., "Inorganic Electronic Spectroscopy", Elsevier Scientific Publ. Co., Amsterdam, **1968**, 2nd. Ed. 1984, Chapter 4.

References

(1) Crutchley, R.J., Kress, N., Lever, A.B.P., J. Am. Chem. Soc., **1983**, 105, 1170.

(2) Haga, M-A., Dodsworth, E.S., Eryavec, G., Seymour, P., Lever, A.B.P., Inorg. Chem., Submitted for publication.

(3) Schilt, A.A., J. Am. Chem. Soc. **1963**, 85, 904.

(4) Peterson, S.H., Demas, J.N., J. Am. Chem. Soc., **1979**, 101, 6571.

(5) Giordano, P.J., Bock, C.R., Wrighton, M.S., J. Am. Chem. Soc. **1978**, 100, 6960.

(6) Giordano, P.J., Bock, C.R., Wrighton, M.S., Interrante, L.V., Williams, R.F.X., J. Am. Chem. Soc., **1977**, 99, 3187.

(7) Hunziger, M., Ludi, A., J. Am. Chem. Soc., **1977**, 99, 7370.

(8) Shriver, D.F., Posner, J., J. Am. Chem. Soc., **1966**, 88, 1672.

(9) Crutchley, R.J., Lever, A.B.P., Inorg. Chem., **1982**, 21, 2276.

(10) Perrin, D.D., Armarego, W.L.F., Perrin, D.R., "Purification of Laboratory Chemicals", 2nd. Edn., Pergamon Press, **1980**.

(11) Saito, H., Fujita, J., Saito, K., Bull. Chem. Soc. Jpn., **1968**, 41, 863.

(12) Burgess, J., J. Organomet. Chem., **1969**, 19, 218.

(13) Walther, D., J. Prakt. Chem., **1974**, 316, 604.

(14) Manuta, D.M., Lees, A.J., Inorg. Chem., **1983**, 22, 3825.

(15) Balk, R.W., Stufkens, D.J., Oskam, A., Inorg. Chim. Acta., **1978**, , 28, 133.

(16) Dodsworth, E.S., Lever, A.B.P., Eryavec, G., Crutchley, R.J., Inorg. Chem., To be submitted.

support. This work is part of a joint ONR Contract with Prof. A.J. Bard, (Austin).

contribution from valence bond forms of the type $[Mo^{+}\text{-}bpz^{-}]$ which is also a description of the MLCT I excited state. Note that since MLCT I is primarily $b_2 \rightarrow b_2^*$, extensive mixing between ground and excited state is permitted by symmetry. A greater mixing of ground and excited state will lead to a smaller difference in bond lengths between these states, as is proposed. It will also lead to greater intensity, since the overlap between ground and excited state wavefunctions is obviously increased.[25]

The BF_3 data support the conclusions reached on the basis of protonation. Band Ia, MLCT I in the mono-BF_3 species, is also more intense and narrower than MLCT I in the parent species (Table V). Band Ib, MLCT I in the di-BF_3 species, is apparently very strong and broad. Its high oscillator strength may be attributed to even greater mixing of metal and bpz orbitals caused by the strongly accepting nature of the two BF_3 groups. The broadness may reflect significant splitting of the d (t_{2g} in O_h) manifold since one of the three d orbitals (b_2) is strongly favoured for mixing, and hence stabilisation relative to the other two.

In conclusion, the protonation and BF_3 data provide evidence for significant mixing between metal and ligand orbitals and the stabilisation of a complex whose back-donating character may be very significant.

Acknowledgements

The authors are indebted to Prof. Ian M. Walker for useful discussions. We also wish to thank the Natural Sciences and Engineering Research Council (Ottawa) and the Office of Naval Research (Washington) for financial

we include a contribution from MLCT Ix, and a very small contribution from the decomposition product (band Ib) to achieve a good fit to the experimental data (Fig. 3). The molar intensity of MLCT Ix is assumed to be about 25% that of MLCT I; it cannot be much larger for then it would be revealed as a shoulder. It is assumed to have the same energy difference from MLCT I as observed in non-polar media. In this approximation, the intensity of band Ib is assumed to be the same as that of band Ia (MLCT I monoprotonated). Its inclusion in the calculated spectrum is necessary to shift the high energy tail of the band I absorption to higher energy with higher acidity. The half-bandwidth of band Ib was estimated from the high acidity data. The various parameters used to simulate the spectrum are shown in Table V. The agreement between calculated gaussian and observed spectra is amazingly good.

Because of the increased decomposition rate, it is not useful to try and simulate the spectra for higher acidities.

The data in Table V merit further consideration. Knowing the molar intensities and half-bandwidths, it is possible to estimate the oscillator strengths and these are also listed. The MLCT I transition in the monoprotonated species (band Ia) is definitively both narrower and much stronger than the corresponding band in the neutral species. The sharper transition provides evidence that the difference in ground and excited state equilibrium distances in this species is smaller than in the parent species. This fact probably reflects a greater degree of covalency in the Mo-N bond with enhanced back-donation because of the greater acceptor power of the now positively charged ligand. The ground state probably has a much greater

contain some contribution from the diprotonated species.

Despite this decomposition it is possible to obtain further useful information from the electronic spectra of the protonated species.

The molecular orbital analysis of this system has been discussed previously.[15,24] The low symmetry (C_{2v}) causes complete loss of degeneracy in the metal d (t_{2g} in O_h) orbitals, resulting in three possible $d \rightarrow \pi^*$ transitions under the MLCT I (band I) envelope. In fact, only two of these are electronically allowed, and are evident in the spectra recorded in polar solvents as pronounced asymmetry in the band I envelope. In non-polar solvents where band narrowing occurs, the second transition appears as a weak higher energy shoulder.[15,16,24] The shoulder and band are assigned as the x-polarised $a_2(d\pi) \rightarrow b_2(bpz\pi^*)$ (band Ix, MLCT Ix) and z-polarised $b_2(d\pi) \rightarrow b_2(bpz\pi^*)$ (MLCT I) transitions respectively.[15]

Fig. 3 shows a computer simulation of the experimental data in Fig. 2a. The gaussians used are shown for one particular spectrum, in Fig. 4. The simulation was obtained in the following manner. The molar intensities and half-bandwidths of the parent species spectrum are known from the spectrum in ethanol. The existence of isosbestic points at low acidities and the comparatively large separation between the band I and band Ia peaks permits the estimation of the corresponding quantities for the monoprotonated species, assuming the absence of any diprotonated species, a good assumption at low acidity.

The spectra are then created using these data and the calculated percentages of parent and monoprotonated species derived from the experimental spectrum. In a second order correction of the calculated data,

base than the ground state since a red shifted band does not appear.[23] This is reasonable if the orbital indeed has nodal planes through the nitrogen atoms.

The well behaved nature of the spectra obtained with BF_3.etherate and the clean reversibility leave little doubt that band Ib in this experiment corresponds with the di-BF_3 adduct, $M(CO)_4(bpz(BF_3)_2)$. This is blue shifted because the presence of one BF_3 group, withdrawing electron density from the bpz ligand, will inhibit binding of the second. Thus the stability constant for binding the second BF_3 unit in the excited state (formally bound to Mo(I)) is less than the corresponding value in the ground state (bound to Mo(0)); hence a blue shift in the Forster scheme.

Band Ib in the higher molarity H_2SO_4 data is not so readily identified. The presence of one proton in the monoprotonated species will inhibit the binding of the second proton to a greater degree than in the BF_3 situation, because of the added positive charge. The second pK_a value for free bipyrazine is -1.35, thus $K_a(2)/K_a(1) = 63$. This ratio is likely to prevail in the carbonyl complex. With this ratio, $pK_a(2)$ = ca -2.0 and essentially no (<5%) diprotonated complex would be seen even at the highest acid concentrations used in this study. Thus either band Ib is extraordinarily intense as MLCT I of the diprotonated species, or it is not associated with the diprotonated species. Since it increases slightly in intensity with time, and band I is not cleanly reproduced upon dilution or neutralisation, we suggest that band Ib arises at least in part, from a decomposition product. The band Ib envelope, however, probably does

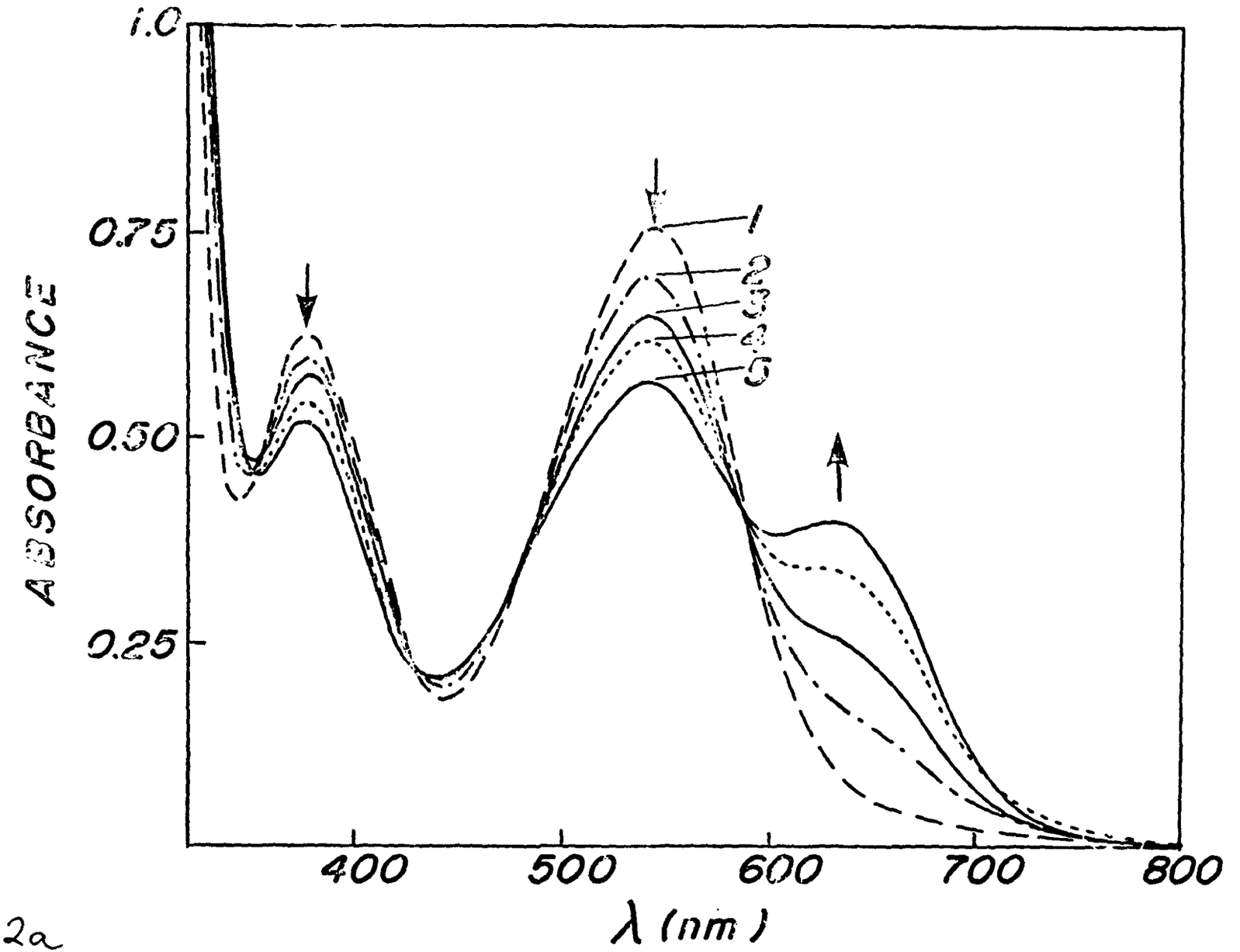

Fig 2a

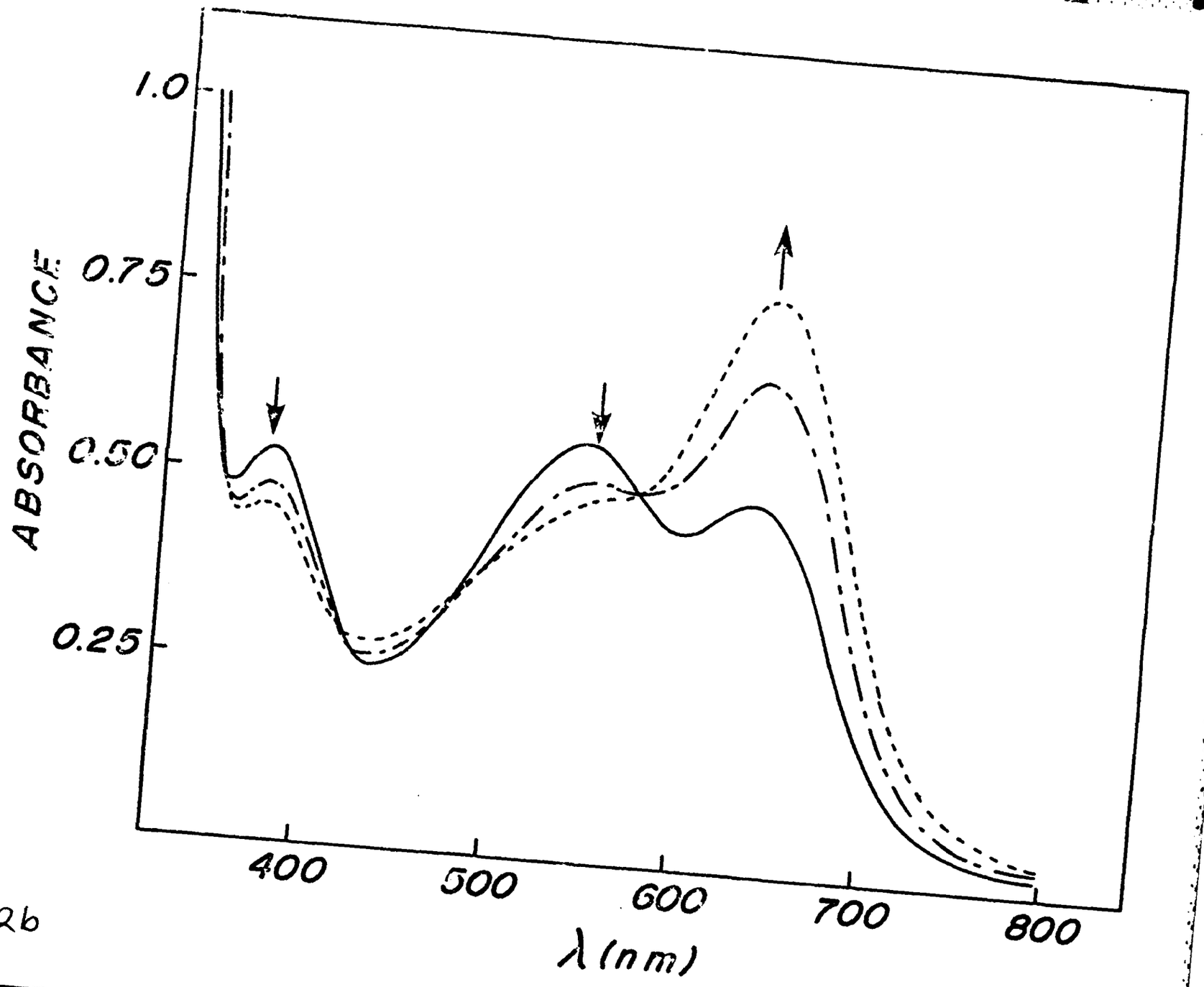

Fig 2b

ISOSBESTIC PLOTS 13/7/84

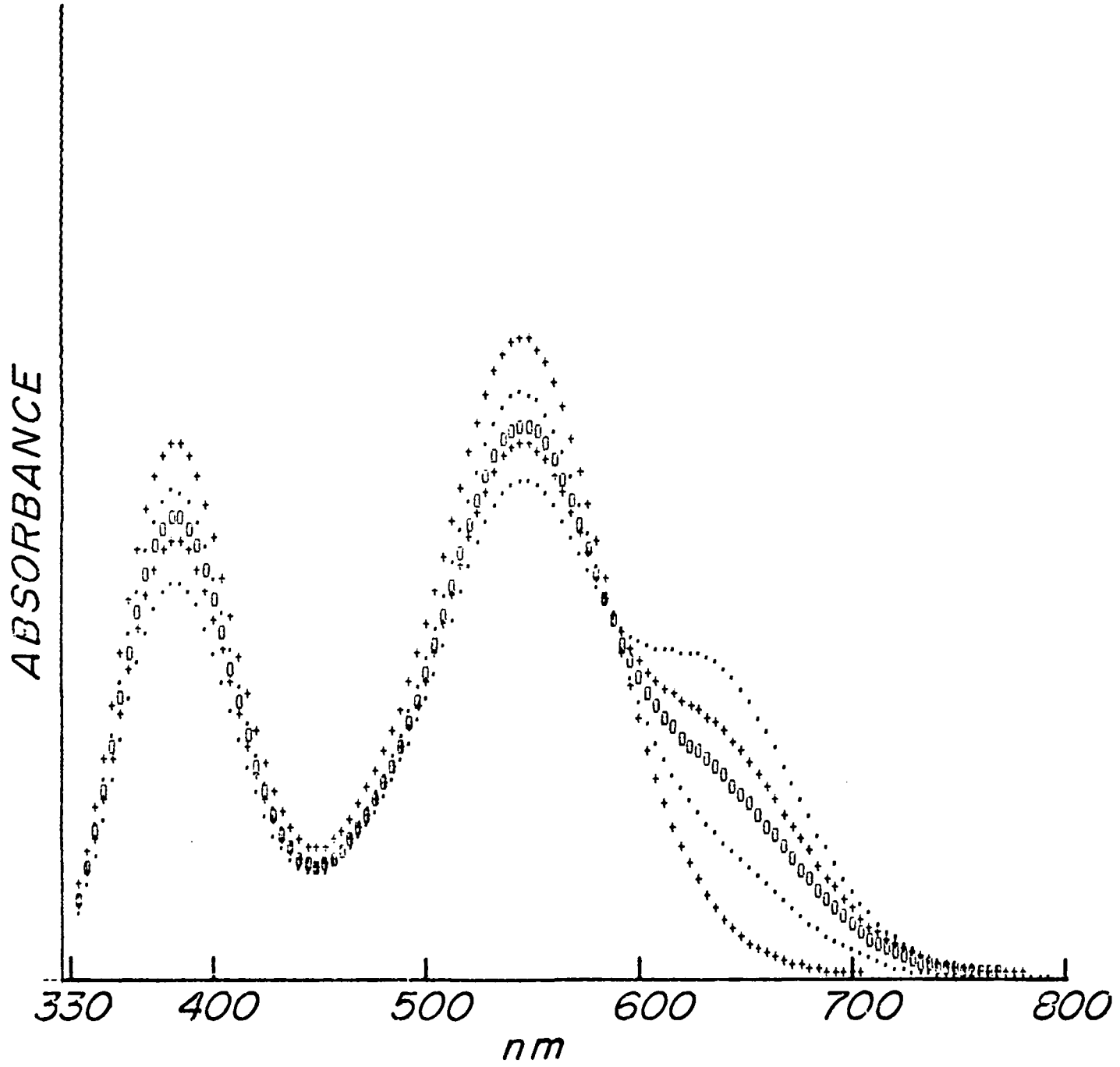

Fig 3

• GAUSSIAN ANALYSIS 12/7/84

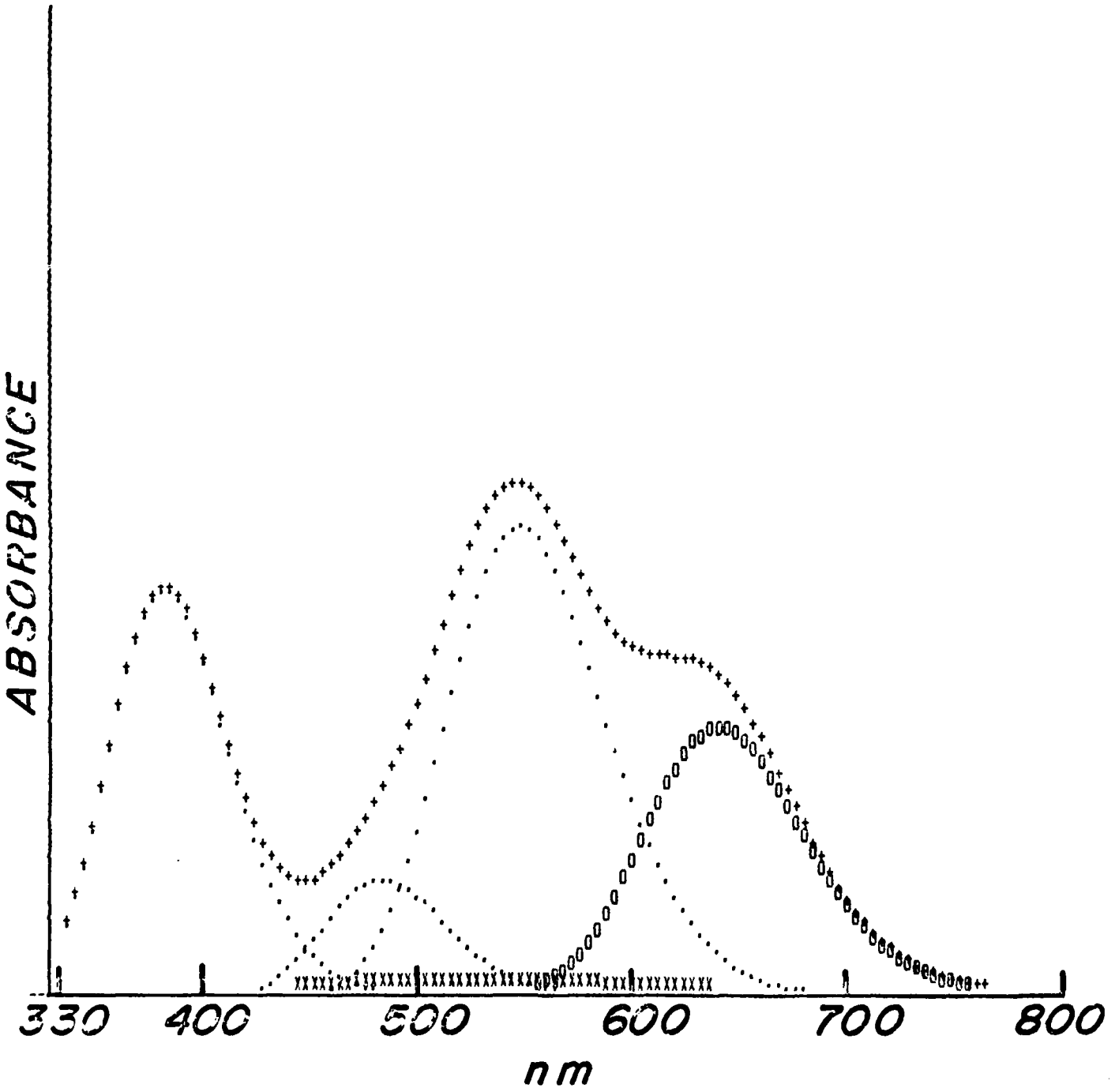

Fig 4.

DL/413/83/01
GEN/413-2

TECHNICAL REPORT DISTRIBUTION LIST, GEN

	No. Copies
Office of Naval Research Attn: Code 413 800 N. Quincy Street Arlington, Virginia 22217	2
Dr. Bernard Douda Naval Weapons Support Center Code 5042 Crane, Indiana 47522	1
Commander, Naval Air Systems Command Attn: Code 310C (H. Rosenwasser) Washington, D.C. 20360	1
Naval Civil Engineering Laboratory Attn: Dr. R. W. Drisko Port Hueneme, California 93401	1
Defense Technical Information Center Building 5, Cameron Station Alexandria, Virginia 22314	12
DTNSRDC Attn: Dr. G. Bosmajian Applied Chemistry Division Annapolis, Maryland 21401	1
Dr. William Tolles Superintendent Chemistry Division, Code 6100 Naval Research Laboratory Washington, D.C. 20375	1
Dr. David Young Code 334 NORDA NSTL, Mississippi 39529	1
Naval Weapons Center Attn: Dr. A. B. Amster Chemistry Division China Lake, California 93555	1
Scientific Advisor Commandant of the Marine Corps Code RD-1 Washington, D.C. 20380	1
U.S. Army Research Office Attn: CRD-AA-IP P.O. Box 12211 Research Triangle Park, NC 27709	1
Mr. John Boyle Materials Branch Naval Ship Engineering Center Philadelphia, Pennsylvania 19112	1
Naval Ocean Systems Center Attn: Dr. S. Yamamoto Marine Sciences Division San Diego, California 91232	1

DL/413/83/01
359/413-2

ABSTRACTS DISTRIBUTION LIST, 359/627

Dr. Paul Delahay
Department of Chemistry
New York University
New York, New York 10003

Dr. P. J. Hendra
Department of Chemistry
University of Southampton
Southampton S09 5NH
United Kingdom

Dr. T. Katan
Lockheed Missiles and
Space Co., Inc.
P.O. Box 504
Sunnyvale, California 94088

Dr. D. N. Bennion
Department of Chemical Engineering
Brigham Young University
Provo, Utah 84602

Mr. Joseph McCartney
Code 7121
Naval Ocean Systems Center
San Diego, California 92152

Dr. J. J. Auborn
Bell Laboratories
Murray Hill, New Jersey 07974

Dr. Joseph Singer, Code 302-1
NASA-Lewis
21000 Brookpark Road
Cleveland, Ohio 44135

Dr. P. P. Schmidt
Department of Chemistry
Oakland University
Rochester, Michigan 48063

Dr. H. Richtol
Chemistry Department
Rensselaer Polytechnic Institute
Troy, New York 12181

Dr. R. A. Marcus
Department of Chemistry
California Institute of Technology
Pasadena, California 91125

Dr. E. Yeager
Department of Chemistry
Case Western Reserve University
Cleveland, Ohio 44106

Dr. C. E. Mueller
The Electrochemistry Branch
Naval Surface Weapons Center
White Oak Laboratory
Silver Spring, Maryland 20910

Dr. Sam Perone
Chemistry & Materials
Science Department
Lawrence Livermore National Laboratory
Livermore, California 94550

Dr. Royce W. Murray
Department of Chemistry
University of North Carolina
Chapel Hill, North Carolina 27514

Dr. B. Brummer
EIC Incorporated
111 Downey Street
Norwood, Massachusetts 02062

Dr. Adam Heller
Bell Laboratories
Murray Hill, New Jersey 07974

Electrochimica Corporation
Attn: Technical Library
2485 Charleston Road
Mountain View, California 94040

Library
Duracell, Inc.
Burlington, Massachusetts 01803

Dr. A. B. Ellis
Chemistry Department
University of Wisconsin
Madison, Wisconsin 53706

Dr. Manfred Breiter
Institut fur Technische Elektrochemie
Technischen Universitat Wien
9 Getreidemarkt, 1160Wien
AUSTRIA

ABSTRACTS DISTRIBUTION LIST, 359/627

Dr. M. Wrighton
Chemistry Department
Massachusetts Institute
of Technology
Cambridge, Massachusetts 02139

Dr. B. Stanley Pons
Department of Chemistry
University of Utah
Salt Lake City, Utah 84112

Donald E. Mains
Naval Weapons Support Center
Electrochemical Power Sources Division
Crane, Indiana 47522

S. Ruby
DOE (STOR)
M.S. 6B025 Forrestal Bldg.
Washington, D.C. 20595

Dr. A. J. Bard
Department of Chemistry
University of Texas
Austin, Texas 78712

Dr. Janet Osteryoung
Department of Chemistry
State University of New York
Buffalo, New York 14214

Dr. Donald W. Ernst
Naval Surface Weapons Center
Code R-33
White Oak Laboratory
Silver Spring, Maryland 20910

Mr. James R. Moden
Naval Underwater Systems Center
Code 3632
Newport, Rhode Island 02840

Dr. Bernard Spielvogel
U.S. Army Research Office
P.O. Box 12211
Research Triangle Park, NC 27709

Dr. Aaron Fletcher
Naval Weapons Center
Code 3852
China Lake, California 93555

Dr. M. M. Nicholson
Electronics Research Center
Rockwell International
3370 Miraloma Avenue
Anaheim, California

Dr. Michael J. Weaver
Department of Chemistry
Purdue University
West Lafayette, Indiana 47907

Dr. R. David Rauh
EIC Laboratories, Inc.
111 Downey Street
Norwood, Massachusetts 02062

Dr. Aaron Wold
Department of Chemistry
Brown University
Providence, Rhode Island 02192

Dr. Martin Fleischmann
Department of Chemistry
University of Southampton
Southampton SO9 5NH ENGLAND

Dr. R. A. Osteryoung
Department of Chemistry
State University of New York
Buffalo, New York 14214

Dr. Denton Elliott
Air Force Office of Scientific
Research
Bolling AFB
Washington, D.C. 20332

Dr. R. Nowak
Naval Research Laboratory
Code 6170
Washington, D.C. 20375

Dr. D. F. Shriver
Department of Chemistry
Northwestern University
Evanston, Illinois 60201

Dr. Boris Cahan
Department of Chemistry
Case Western Reserve University
Cleveland, Ohio 44106

DL/413/83/01
359/413-2

ABSTRACTS DISTRIBUTION LIST, 359/627

Dr. David Aikens
Chemistry Department
Rensselaer Polytechnic Institute
Troy, New York 12181

Dr. A. B. P. Lever
Chemistry Department
York University
Downsview, Ontario M3J1P3

Dr. Stanislaw Szpak
Naval Ocean Systems Center
Code 6343, Bayside
San Diego, California 95152

Dr. Gregory Farrington
Department of Materials Science
and Engineering
University of Pennsylvania
Philadelphia, Pennsylvania 19104

M. L. Robertson
Manager, Electrochemical
and Power Sources Division
Naval Weapons Support Center
Crane, Indiana 47522

Dr. T. Marks
Department of Chemistry
Northwestern University
Evanston, Illinois 60201

Dr. Micha Tomkiewicz
Department of Physics
Brooklyn College
Brooklyn, New York 11210

Dr. Lesser Blum
Department of Physics
University of Puerto Rico
Rio Piedras, Puerto Rico 00931

Dr. Joseph Gordon, II
IBM Corporation
K33/281
5600 Cottle Road
San Jose, California 95193

Dr. Hector D. Abruna
Department of Chemistry
Cornell University
Ithaca, New York 14853

Dr. D. H. Whitmore
Department of Materials Science
Northwestern University
Evanston, Illinois 60201

Dr. Alan Bewick
Department of Chemistry
The University of Southampton
Southampton, SO9 5NH ENGLAND

Dr. E. Anderson
NAVSEA-56Z33 NC #4
2541 Jefferson Davis Highway
Arlington, Virginia 20362

Dr. Bruce Dunn
Department of Engineering &
Applied Science
University of California
Los Angeles, California 90024

Dr. Elton Cairns
Energy & Environment Division
Lawrence Berkeley Laboratory
University of California
Berkeley, California 94720

Dr. D. Cipris
Allied Corporation
P.O. Box 3000R
Morristown, New Jersey 07960

Dr. M. Philpott
IBM Corporation
5600 Cottle Road
San Jose, California 95193

Dr. Donald Sandstrom
Boeing Aerospace Co.
P.O. Box 3999
Seattle, Washington 98124

Dr. Carl Kannewurf
Department of Electrical Engineering
and Computer Science
Northwestern University
Evanston, Illinois 60201

Dr. Richard Pollard
Department of Chemical Engineering
University of Houston
4800 Calhoun Blvd.
Houston, Texas 77004

ABSTRACTS DISTRIBUTION LIST, 359/627

Dr. Robert Somoano
Jet Propulsion Laboratory
California Institute of Technology
Pasadena, California 91103

Dr. Johann A. Joebstl
USA Mobility Equipment R&D Command
DRDME-EC
Fort Belvoir, Virginia 22060

Dr. Judith H. Ambrus
NASA Headquarters
M.S. RTS-6
Washington, D.C. 20546

Dr. Albert R. Landgrebe
U.S. Department of Energy
M.S. 6B025 Forrestal Building
Washington, D.C. 20595

Dr. J. J. Brophy
Department of Physics
University of Utah
Salt Lake City, Utah 84112

Dr. Charles Martin
Department of Chemistry
Texas A&M University
College Station, Texas 77843

Dr. H. Tachikawa
Department of Chemistry
Jackson State University
Jackson, Mississippi 39217

Dr. Theodore Beck
Electrochemical Technology Corp.
3935 Leary Way N.W.
Seattle, Washington 98107

Dr. Farrell Lytle
Boeing Engineering and
Construction Engineers
P.O. Box 3707
Seattle, Washington 98124

Dr. Robert Gotscholl
U.S. Department of Energy
MS G-226
Washington, D.C. 20545

Dr. Edward Fletcher
Department of Mechanical Engineering
University of Minnesota
Minneapolis, Minnesota 55455

Dr. John Fontanella
Department of Physics
U.S. Naval Academy
Annapolis, Maryland 21402

Dr. Martha Greenblatt
Department of Chemistry
Rutgers University
New Brunswick, New Jersey 08903

Dr. John Wasson
Syntheco, Inc.
Rte 6 - Industrial Pike Road
Gastonia, North Carolina 28052

Dr. Walter Roth
Department of Physics
State University of New York
Albany, New York 12222

Dr. Anthony Sammells
Eltron Research Inc.
4260 Westbrook Drive, Suite 111
Aurora, Illinois 60505

Dr. W. M. Risen
Department of Chemistry
Brown University
Providence, Rhode Island 02192

Dr. C. A. Angell
Department of Chemistry
Purdue University
West Lafayette, Indiana 47907

Dr. Thomas Davis
Polymer Science and Standards
Division
National Bureau of Standards
Washington, D.C. 20234

Ms. Wendy Parkhurst
Naval Surface Weapons Center R-33
Silver Spring, Maryland 20910

END

FILMED

5-85

DTIC